CYBER
Pharmacodia AI

CYBER AIDD

WEEKLY REPORT

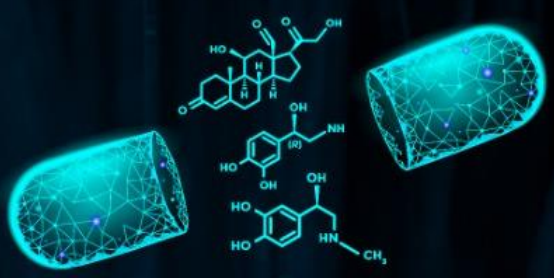

Cyber-AIDD analysis of the discovery and optimization of G-5758, a highly potent and selective oral IRE1α kinase inhibitor developed by Genentech

(*Reference from: Journal of Medicinal Chemistry, 2024, 67,11,8708-8729*)

PART-I

Cyber-AIDD analysis of the discovery and optimization of G-5758, a highly potent and selective oral IRE1α kinase inhibitor developed by Genentech

(Reference from: Journal of Medicinal Chemistry, 2024, 67,11,8708-8729)

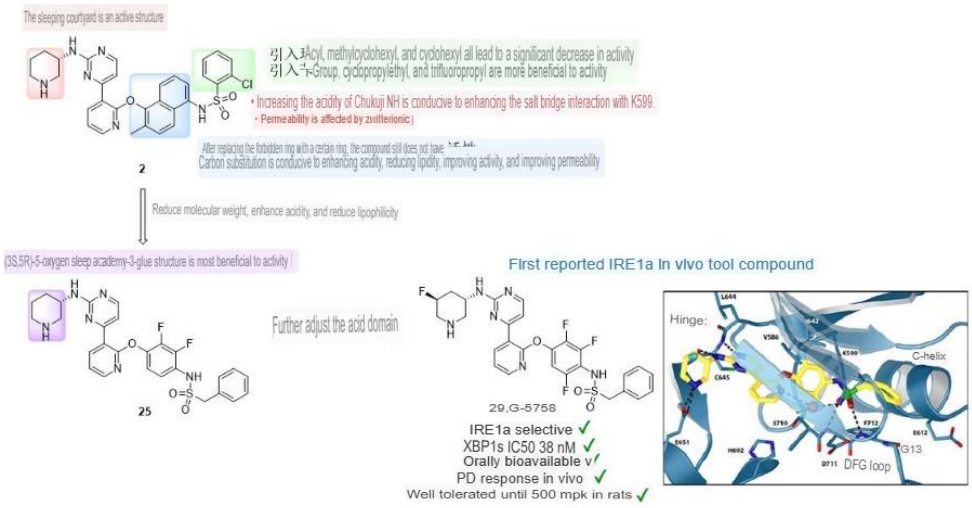

The lack of highly selective and safe in vivo tool has greatly limited the evaluation of IRE1α as a feasible target for the treatment of multiple myeloma (MM). The research team of Genentech in the United States optimized the structure of IRE1α kinase inhibitors reported in the literature and found a group of IRE1α kinase inhibitors with good in vitro safety and oral administration by reducing lipid solubility, molecular weight and alkalinity to improve physical and chemical properties.BioavailabilityThe researchers obtained a highly effective, highly selective and safe IRE1α tool molecule, G-5758. In a multiple myeloma model (KMS-11), the XBP1s level showed that G-5758 exhibited a pharmacodynamic effect comparable to that of IRE1 knockout.

Pharmacodia CyberSAR system provides in-depth analysis of IRE1α kinase inhibitor molecules. The system displays active molecules related to the target through *clustered structure views* and *original structure views*, and presents *potential hits* in the form of a timeline during the research and development stage. In addition, CyberSAR also provides *visual analysis of indications* and *experimental designs* to help R&D personnel quickly obtain target structure information and open up research ideas. Although CyberSAR was not used in the initial development of the molecule in this case, it shows great application potential in analyzing and optimizing drug molecules.

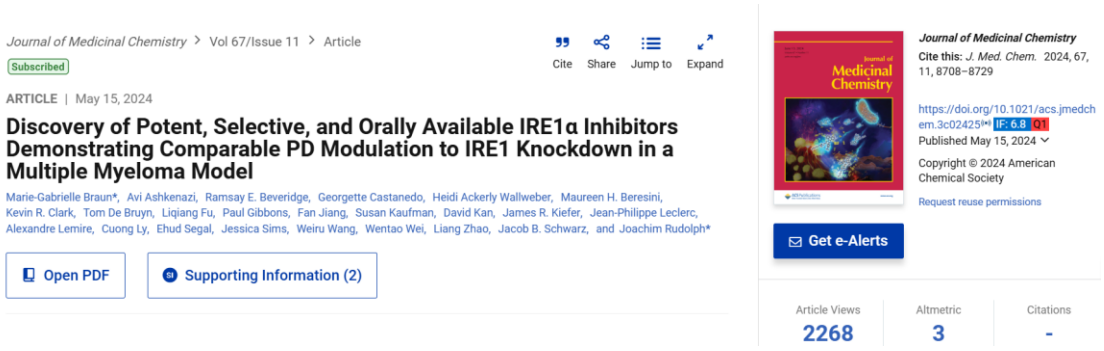

PART-II

Background

The endoplasmic reticulum (ER) is the folding factory for secretory and membrane proteins in eukaryotic cells. When the protein folding burden of the ER exceeds its folding capacity, ER stress will occur. At this time, three transmembrane "sensors" on the ER membrane (IRE1, PERK and ATF6) pass, A series of signal transduction pathways from the ER to the nucleus are initiated to enhance the ER protein folding capacity, stop most protein translation processes, or accelerate protein degradation. These cellular events are collectively referred to as the unfolded protein response (UPR). When the stress intensity exceeds the adaptive range of the UPR, the UPR triggers apoptosis. Multiple myeloma (MM) is a malignant disease characterized by abnormal proliferation of clonal plasma cells. Althoughat presentTreatment and prognosis of multiple myeloma (MM)haveSignificant improvements have been made, but existing therapies often Initiation Drug resistance, most MM patients will eventually experience disease recurrence and progression. IRE1α is located in ER trans membrane protein, can Promotes plasma cell differentiation and immunoglobulin secretion, In the development of MM have Important role. IRE1α Endoplasmic reticulum tubular domain, transmembrane domain and cytoplasmic kinase-RNase Module composition. IRE1α phosphorylation controls its oligomerization and RNaseActivation, thereby through unconventional splicing Pre-mRNA production transcription factor XBP1s, on the other hand Through IRE1-dependent degradation (RIDD) Cutting ER-targeted mRNAs.

Previous studies haveIRE1α is a potential therapeutic target for MM, as allosteric inhibition of RNase via the kinase ATP-binding pocket blocks the growth of MM tumor xenografts in vitro and in vivo. The IRE1α kinase domain is an effective lever for small molecule inhibition of this bifunctional enzyme in vitro and in vivo.The study found thatIRE1α kinase inhibitionThe agent can beDoes not affect normal bone marrow cellsIn the caseSelectively reduce the viability of malignant plasma cells isolated from newly diagnosed or relapsed MM patients after treatment,This provides an important tool for early preclinical research.Researchers onIRE1α kinase inhibitorsThe structure has been optimized to improve Physicochemical properties, Pharmacological properties and safety, This provides important insights into the clinical translation of IRE1α targeted therapyin accordance with.

Results and Discussion

Structure-activity relationship analysis

At present, relevant literature has reported a variety of IRE1α kinase inhibitors, such as naphthalene selective kinase inhibitors 1 and 2 developed by Amgen. However, due to their high toxicity, these compounds cannot be studied in vivo. For example, compound 2 is prone to off-target effects, which is related to its high lipophilicity and alkalinity. In addition, compound 2 has poor permeability, resulting in low solubility and oral bioavailability. Analysis found that these reported IRE1α kinase inhibitors are generally slender in shape and have high molecular weight.The crystal structure of compound 2 shows that IRE1 Key interactions include The salt bridge interaction between piperidine and E651, the interaction with C645, and the salt bridge interaction between sulfonamide and K599, compared with the apolipoprotein structure, it can be observed that the αC-helix shift and the Glu-Lys salt bridge are broken.

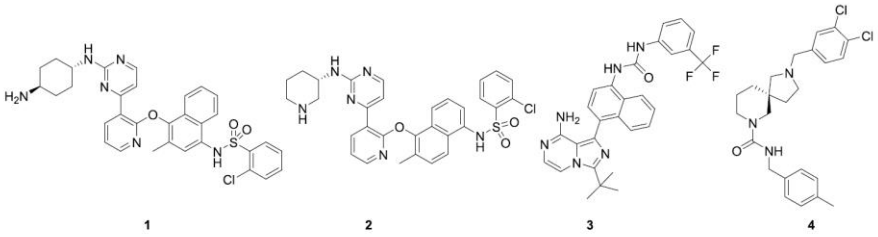

1 2 3 4

	IRE1α-TR-FRET IC_{50} (nM)	IRE1α-RNase IC_{50} (nM)	XBP1s-luc IC_{50} (nM)	# Kinases >50%, >75% [a]	Promiscuity @ 10 μM[b]	cLogP/cpKa[c] (MA)[c]/cpKa(MB)[d]
1	0.85	4.2	57	11,5	33%	7.2 / 7.6 / 10.5
2	0.48	9.2	40	3,1	42%	6.5 / 7.5 / 9.2
3	36	200	180	81, 61	25%	6.2 / -- / 3.2
4	660	46	5900	0, 0	31%	7.9 / 6.8 / --

Figure 1. Reported IRE1α kinase inhibitors. [a]Of 218 kinases tested excluding IRE1α and IRE1β at [IRE1α inhibitor] = 1 μM. [b]CEREP secondary pharmacology: Percentage of off-target hits with >50% binding or inhibition at [IRE1α inhibitor] = 10 μM (out of a total of 40 tested). [c]Data are shown for the most acidic center. [d]Data are shown for the most basic center. [e]Calculated log P and calculated pK_a using Moka software from Molecular Discovery.

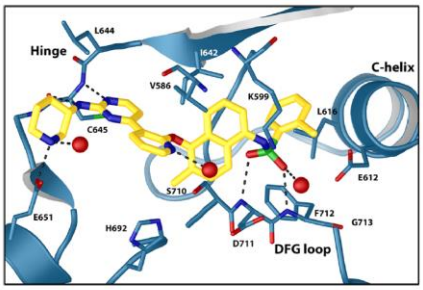

Figure 2. X-ray cocrystal structure of compound **2** (yellow) bound to hIRE1 (blue, PDB code 6urc, 1.90 Å).

In order to solve the off-target problem of compound 2, the researchers first modified the structure of the piperidine part. When piperidine was replaced with amino (5) or pyrazole (9), the activity of the compound was completely lost; the introduction of a lactam structure (6) or the replacement of the piperidine N atom with an O atom (7) resulted in a significant decrease in activity; the activity of the enantiomer 8 of compound 2 was significantly reduced; difluorinated substitution at the piperidine 5 position (10) or trifluoroethylation of the piperidine nitrogen atom (11) resulted in a significant decrease in activity, indicating that piperidine is a necessary structure for activity.

Table 1. Piperidine SAR in the Naphthalene Series

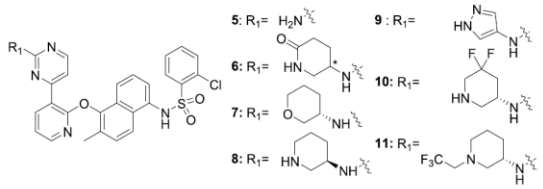

	IRE1α-HTRF IC_{50} (nM)	IRE1α-RNase IC_{50} (nM)	XBP 1s-luc IC_{50} (nM)	cLog *P*/cpK_a[c]
5	>1000	>10 000	32 000	5.5/3.5
6[b]	65	2100	9000	5.6/3.3
7	42	>10 000	26 000	6.8/2.3
8	46	420	2300	6.5/9.2
9	>1000	>10 000	>50 000	6.7/3.6
10	17	250	2300	6.6/6.3
11	>1000	>10 000	28 000	7.8/4.9

[a]Data represent a geometric mean of >2 separate determinations. [b]Data are shown for the most potent enantiomer. [c]Calculated log *P* and calculated pK_a using Moka software from Molecular Discovery. Data are shown for the most basic center.

For the sulfonamide part, the introduction of cyclohexyl (12), methylcyclohexyl (13) and cyclopentyl (14) structures all led to a significant decrease in activity; the activity of compound 15 containing a benzylsulfonamide structure was 2 times higher than that of compound 2, which may be due to the effective shift of the α C-helix by the introduction of the benzyl group; the compounds containing propylsulfonamide (16) and cyclopropylethylsulfonamide (17) structures were more active; the introduction of trifluoropropyl (18) enhanced the acidity of the compound (cpKa = 7.6) and increased its activity by 4 times compared with compound 17, and it is speculated that increasing the acidity of the sulfonamide NH will help to enhance its salt bridge interaction with K599. Next, the researchers synthesized fluoronaphthalene compounds to further enhance the acidity, and the activity of compound 19 was 3 times higher than that of compound 18. The activity of methylnaphthalene compound 20 was also significantly improved compared with compound 18, which may be due to the presence of methyl groups promoting the formation of hydrophobic interactions. Among these compounds, compound 19 has lower promiscuity, which may be related to its lower lipophilicity. However, the permeability of these compounds is still generally low.

Table 2. Sulfonamide SAR in the Naphthalene Series

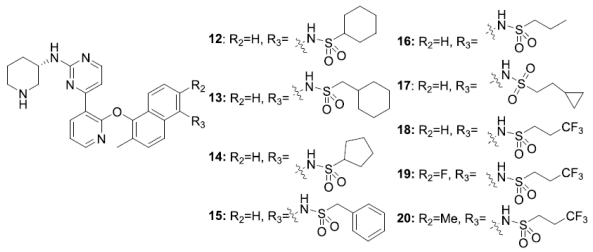

	IRE1α-HTRF IC_{50} (nM)	IRE1α-RNase IC_{50} (nM)	XBP 1s-luc IC_{50} (nM)	cLog *P*/cpK_a[c]
12	2.2	17	200	6.3/8.6
13	2.1	24	1300	6.3/8.3
14	3.3	13	200	6.5/8.6
15[b]	0.35	17	18	5.8/8.6
16	4.7	6.3	140	5.2/8.3
17	1.8	19	300	5.5/8.7
18	1.1	8.7	84	5.5/7.6
19	0.39	2.1	35	5.1/6.8
20	0.66	3.3	42	5.4/7.7

[a]Data represent the geometric mean of >2 separate determinations. [b]IRE1α-TR-FRET IC_{50} for **15** is close to the bottom of the assay. [c]Calculated log *P* and calculated pK_a using Moka software from Molecular Discovery. Data are shown for the most acidic center when measured pK_a correlates well with cpK_a.

For the naphthalene ring, the 1,4-naphthalene ring substituted (21) compound also has better activity. Modeling found that the benzene ring in the 1,4-naphthalene ring has a significant effect on the activity of the compound.Binding to IRE1α proteinnoneSignificant Contribution. Replace the naphthalene ring with a benzene ring (2**2**), the compound still has a certain activity.**3**, 2**4**, 2**5**, 2**6**) can enhance the acidity and activity of the compounds. Compared with compound 2, these

compoundsLower lipophilicity and higher permeability, indicating that the permeability is affected by zwitterions. Then, a methyl group (2**7**, 2**8**) had no significant improvement on activity.

Table 3. Core SAR

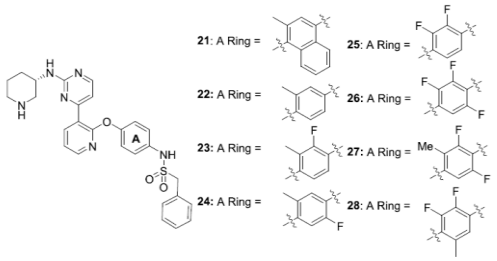

	IRE1α-HTRF IC_{50} (nM)	IRE1α-RNase IC_{50} (nM)	XBP 1s-luc IC_{50} (nM)	cLog *P*/cpK_a[c]	MDCK A to B P_{app} (10^{-6} cm/s)
21	0.38	5.4	31	5.8/8.6	ND
22	29	170	4400	4.7/8.3	ND
23	1.8	24	330	4.9/7.6	2.0
24	2.1	14	310	4.7/7.6	ND
25	0.98	2.9	88	4.5/7.0	2.1
26	3.1	4.5	47	4.1/6.3	1.4
27	0.29	2.9	37	4.5/6.8	1.1
28	0.29	4.5	44	4.9/7.2	2.8

[a]Data represent a geometric mean of >2 separate determinations. [b]Data are shown for the most potent enantiomer. [c]Calculated log *P* and calculated pK_a using Moka software from Molecular Discovery. Data are shown for the most acidic center.

For the piperidine part, the introduction of (S)-F (29, G-5758) at the 5-position weakened the basicity of the compound, improved the permeability, and its activity was 10 times that of its R isomer (30), indicating that the (3S,5R)-5-fluoropiperidin-3-amine structure is more favorable for activity. 5-Fluoro-5-methylpiperidin substituted compounds 31 and 5-fluoromethylpiperidin substituted compounds 32 also have good activity and low promiscuity. Replacing benzylsulfonamide with trifluoropropylsulfonamide or propylsulfonamide resulted in a significant decrease in activity.

Table 4. Piperidine SAR in the Phenoxy Series

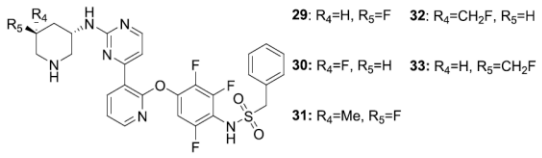

	IRE1α-HTRF IC_{50} (nM)	IRE1α-RNase IC_{50} (nM)	XBP 1s-luc IC_{50} (nM)	cLog *P*/cpK_a[c]	MDCK A to B P_{app} (10^{-6} cm/s)	promiscuity @ 10 μM[d]
29	0.27	4.3	38	3.9/8.1	8.7	2.4%
30	2.0	23	2700	3.9/8.1	ND	ND
31	0.59	7.4	22	4.1/8.2	7.3	2.4%
32	0.26	5.2	32	4.0/8.2	2.6	2.4%
33	0.78	15	540	4.0/8.2	ND	ND

[a]Data represent a geometric mean of >2 separate determinations. [b]Data are shown for the most potent enantiomer. [c]Calculated log *P* and calculated pK_a using Moka software from Molecular Discovery. Data are shown for the most basic center. [d]CEREP secondary pharmacology profiling. Percentage of off-target hits with >50% inhibition at [IRE1α inhibitor] = 10 μM (out of a total of 40 tested).

Compound 29Determination of molecules for in vivo studies

The co-crystal structure of compound 29 with IRE1α showed that its binding mode was similar to that of compound 2. The aminopyrimidine part formed a hydrogen bond with C645; the piperidine part formed a salt bridge with E651, which was crucial to the activity and selectivity of the compound; the binding of 29 to IRE1α shifted the C-helix and destroyed the salt bridge interaction between E612 and K599; the sulfonamide part formed a pair of hydrogen bonds with the DFG main chain atoms, supporting the benzyl part on the shifted C-helix; the pyridine ring was bonded to the K599 side chain through a water molecule.and the β-sheet backbone of the P-loopProduce interactions.

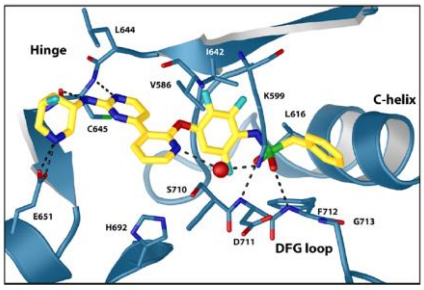

Figure 3. X-ray cocrystal structure of compound **29** (yellow carbons) in hIRE1 (blue, PDB code 8UVL).

Compared with other IRE1 inhibitors, compound 29 has the advantages of high efficiency, high selectivity, high oral bioavailability, and better overall properties, making it an ideal molecule for in vivo studies.

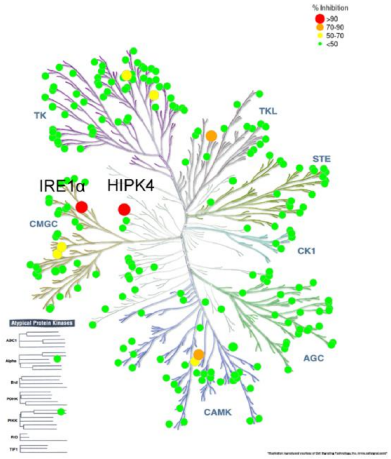

Figure 4. Kinase inhibitory activities of compound **29** at 1 μM in a panel of 220 kinases.

Table 5. Solubility Data, In Vitro ADME Data, and Mouse PK Parameters for 29, 31, and 32

	in vitro				in vivo[c]				
	kinetic solubility (μM)[a]	LM[b] CL_{hep} (mL/min/kg)	Heps[c] CL_{hep} (mL/min/kg)	PPB[d] (%)	dose (mg/kg) /route	CL (mL/min/kg)	V_{ss} (L/kg)	$t_{1/2}$ (h)	%F[f]
29	65	76	50	97.1	1 (IV)/10 (PO)	33.9	1.05	0.55	149
31	46	65	44	99.1	1 (IV)/10 (PO)	19.9	1.04	1.56	109
32	28	49	33	97.1	1 (IV)/10 (PO)	61.4	3.51	0.75	36

[a]Experiment run at pH 7.4. [b]Liver microsomal clearance. [c]Hepatocyte clearance. [d]Plasma protein binding. [e]Dosed IV (bolus) at 1 mg/kg as a solution in dimethyl sulfoxide (DMSO)/PEG400/water (10/35/55) or PO at 10 mg/kg as a suspension in DMSO/PEG400/water (10/50/40), data reported as means of n = 3 CD-1 female mice. [f]%F is bioavailability.

In vivo safety, pharmacodynamics and pharmacokinetic evaluation of compound 29

Rats were orally administered with compound 29 twice a day for 7 days, with the highest dose of 500 mg/kg being well tolerated.

In vivo pharmacodynamic (PD) evaluation was performed using KMS-11 cell-based bDNA technology, and the results showed that the IC50 value of compound 29 was 64 nM at 24 h.

Table 6. Cellular PD Profile of 29 in Two Different Mechanistic Cell Assay Formats

	IC_{50} or IC_{90} [μM]	IC_{50} or IC_{90} (FCS binding corrected) [μM][a]
XBP1s reporter IC_{50} (5 h)	0.032	0.0039
XBP1s bDNA IC_{50} (24 h)	0.064	0.0078
XBP1s bDNA IC_{90} (24 h)	0.65	0.079

[a]IC_{50} or IC_{90} values accounting for measured protein binding in the assay medium containing 10% fetal calf serum (FCS) protein.

The results of pharmacokinetic evaluation showed that compound 29 had a dose-dependent exposure, and 250 mg/kg BID could provide the plasma exposure level required for PD evaluation.

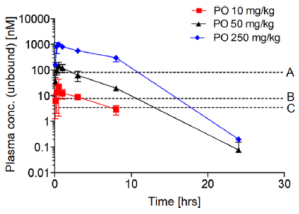

Figure 5. Exposure curves for mouse pharmacokinetic studies using three different oral doses of **29**. The dotted lines represent the FCS binding-corrected cellular data corresponding to the XBP1s bDNA IC_{90} (A), XBP1s bDNA IC_{50} (B), and XBP1s reporter assay IC_{50} (C). The exposure levels achieved with the 250 mg/kg dose exceed the XBP1s bDNA IC_{90} for 12 h.

Use carry Doxycycline (Dox)-induced resistance to IRE1αshRNA（sh9/8 KMS-11）KMS-11 cells PK/PD study in mice with subcutaneous tumor xenografts showed that Dox-inducedIRE1α knockdownCompound 29 had a strong inhibitory effect on XBP1s for up to 12 hours, which is consistent with its high plasma exposure level, and XBP1 levels rebounded at 16 and 24 hours, which is consistent with the decrease in drug levels in plasma and tumors.Since XBP1 splicing is a key function of IRE1α,Compound 2**9**Really reproducedEffects of IRE1α knockdown on XBP1.

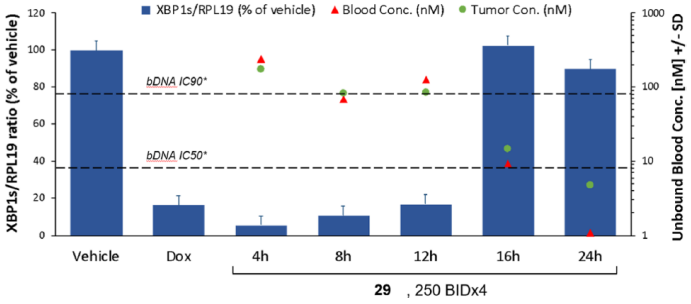

Figure 6. Mouse PK/PD study with **29** in the sh9/8 KMS-11 xenograft model. The blue bars indicate XBP1s levels relative to the vehicle control (left bar, normalized to 100%). The second bar from the left represents the group treated with doxycycline to knockdown IRE1, and the remaining bars signify the XBP1s levels of **29**-treated animals at 4, 8, 12, 16, and 24 h after the last 4 instances of 250 mg/kg BID dosing. Unbound blood and total tumor concentrations at various time points are depicted as red triangles and green circles, respectively, referring to the *y*-axis on the right-hand side of the chart.

Summarize

This study used a structure-based drug design approach to modify the structure of compound 2 reported in the literature to reduce the molecular weight, and discovered compound 25 with good activity and better physicochemical properties and permeability. Then, by optimizing the structure of the sulfonamide and piperidine parts to adjust the acidity and alkalinity of the compound, a highly effective IRE1α inhibitor 29 (G-5758) with good oral bioavailability and low promiscuity was discovered. In vivo studies have shown that G-5758 has a high safety profile and exhibits a pharmacodynamic effect comparable to that of IRE1 knockout in the KMS-11 tumor xenograft model. It is an ideal in vivo tool molecule that can be used to evaluate the therapeutic effect of IRE1α inhibition on multiple myeloma.

source:https://doi.org/10.1021/acs.jmedchem.3c02425

PART-III

1. Pharmacodia CyberSAR combines drug design ideas and mines the active structures reported in literature and patents. Through CyberSAR, researchers can quickly and easily obtain the target structures of interest to them, so as to provide ideas for development. The target IRE1α in this article is given as an example as follows:

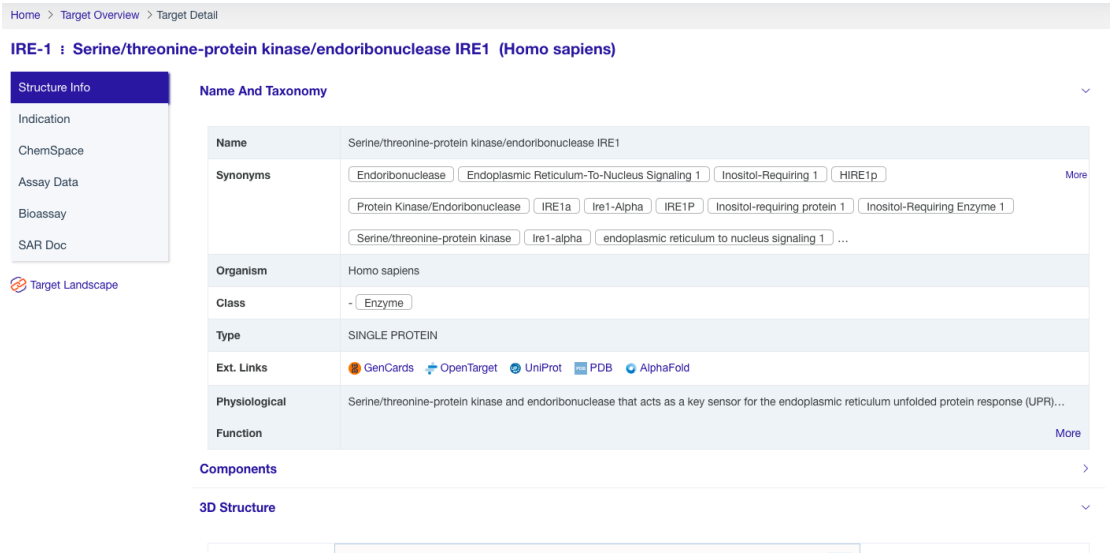

2. In the target interface, select the "Chemical Space" option tab and cascade the "Cluster Structure View" tab to display the molecules with target-related experimental test activities in the literature and patents collected by the CyberSAR platform in the form of "nucleus structure clusters". Among them, the "green font highlights" are the active molecular structures, specific experiments, experimental results and experimental sources with IC50 <1000 nM in in vitro enzyme and cell activity test experiments reported in the literature.

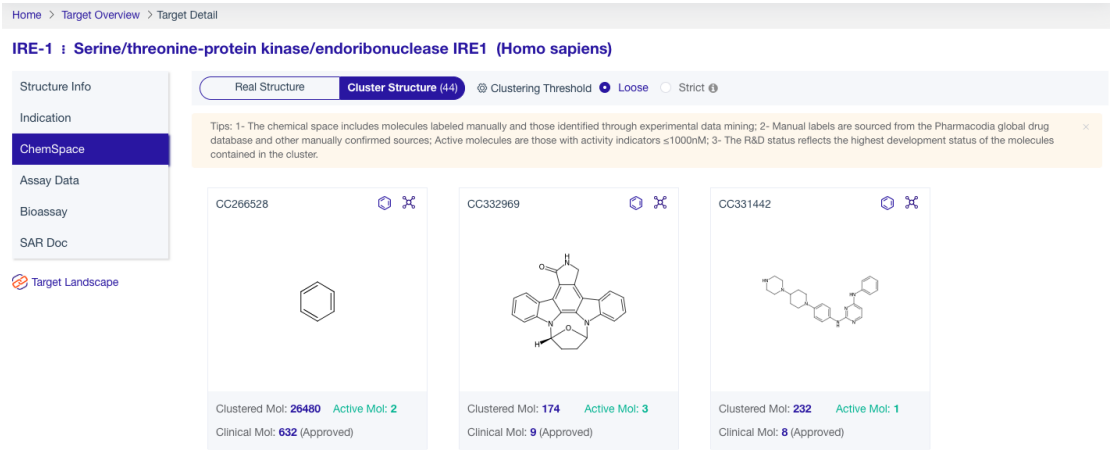

3. In the target interface, select the "Chemical Space" option tab and cascade the "Real Structure View" tab to display the molecules with target-related experimental test activity in the literature collected by the CyberSAR platform in the form of a "R&D stage timeline". The green highlight shows the potential hit.

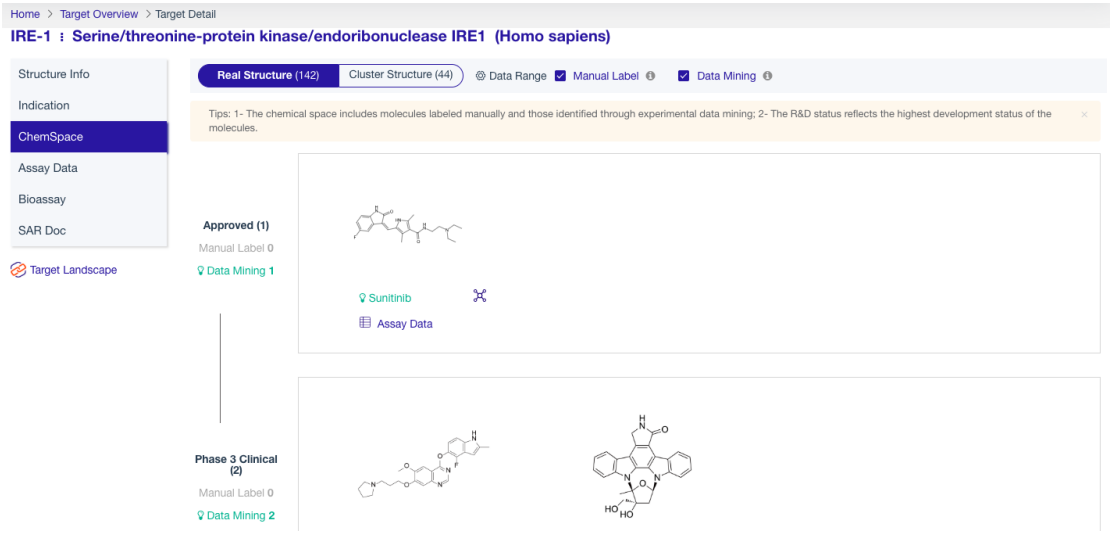

4. Select the "Indications" option label in the target interface to visualize and intuitively analyze the various types of big data currently collected.

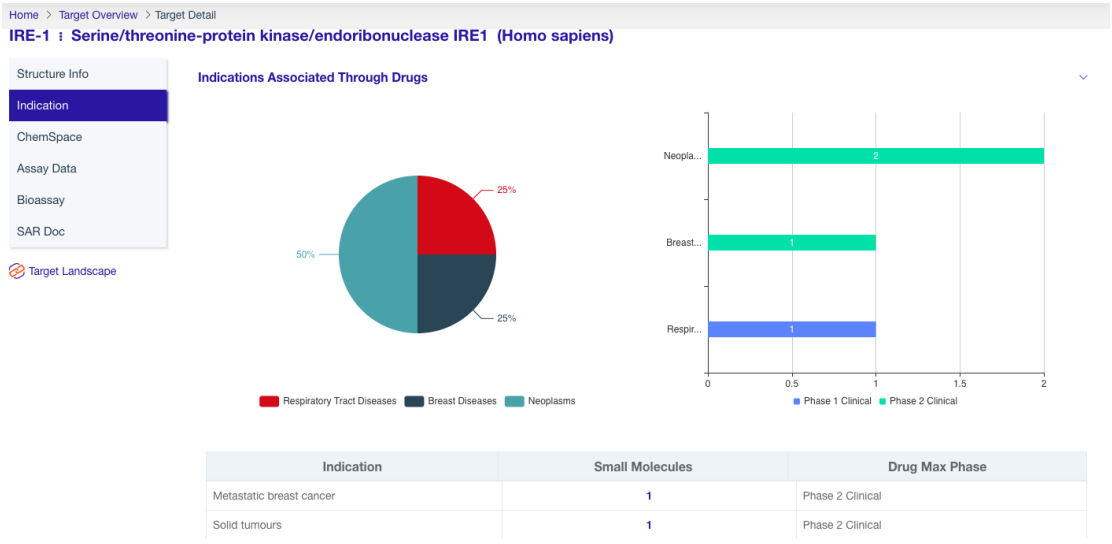

Indication	Small Molecules	Drug Max Phase
Metastatic breast cancer	1	Phase 2 Clinical
Solid tumours	1	Phase 2 Clinical

To Explore Cyber-AIDD further Login on your computer using the below Link

https://cyber.pharmacodia.com/#/homePage

For a Free Trial or for further assistance contact us.

Contact us

Anil Ranadev
+91 9742627845
anil_ranadev@saspinjara.com

Aravind
+91 9619076286
aravind.p@saspinjara.com

Sachin Marihal
+91 9538033363
sachin.marihal@saspinjara.com

Chetan S
+91 7022031061
chetans@saspinjara.com